A Generic Inner-Loop Control Law Structure for Six-Degree-of-Freedom Conceptual Aircraft Design*

Timothy H. Cox† and M. Christopher Cotting‡
NASA Dryden Flight Research Center, Edwards, California, 93523

A generic control system framework for both real-time and batch six-degree-of-freedom (6-DOF) simulations is presented. This framework uses a simplified dynamic inversion technique to allow for stabilization and control of any type of aircraft at the pilot interface level. The simulation, designed primarily for the real-time simulation environment, also can be run in a batch mode through a simple guidance interface. Direct vehicle-state acceleration feedback is required with the simplified dynamic inversion technique. The estimation of surface effectiveness within real-time simulation timing constraints also is required. The generic framework provides easily modifiable control variables, allowing flexibility in the variables that the pilot commands. A direct control allocation scheme is used to command aircraft effectors. Primary uses for this system include conceptual and preliminary design of aircraft, when vehicle models are rapidly changing and knowledge of vehicle 6-DOF performance is required. A simulated airbreathing hypersonic vehicle and simulated high-performance fighter aircraft are used to demonstrate the flexibility and utility of the control system.

Nomenclature

A	=	state matrix
ACT	=	actuator representation
B	=	control matrix
BEST	=	B-matrix estimation
C	=	output matrix
$\dot{cv}$	=	rate of change of control variable with respect to time
D	=	control output matrix
deg	=	degree
dt	=	integration time step
g	=	nondimensional acceleration constant due to gravity
K_{bw}	=	control law bandwidth gain
K_{in}	=	control law stick input gain
M	=	Mach
msec	=	millisecond
NDI	=	nonlinear dynamic inversion
R	=	range to target aircraft, ft
SDI	=	simplified dynamic inversion
s	=	Laplace operator
sec	=	second
u	=	input vector representing control surface effector positions
u_{cmd}	=	input vector representing control surface effector commands
x	=	state vector representing aircraft states
$\dot{x}$	=	rate of change of state vector with respect to time

* The use of trademarks or names of manufacturers is for accurate reporting and does not constitute an official endorsement, either expressed or implied, by the National Aeronautics and Space Administration.

† Aerospace Engineer, Dynamics and Controls Branch, P.O. Box 273/Mail Stop 4840D.
‡ Aerospace Engineer, Dynamics and Controls Branch, P.O. Box 273/Mail Stop 4840D, AIAA Member.

y = output vector representing aircraft output
$\dot{y}$ = rate of change of output vector with respect to time
6-DOF = six-degree-of-freedom
α = angle of attack, deg

Subscripts
m = modeled parameter

I. Introduction

THE preliminary stages of aircraft design typically are characterized by a highly conceptual approach. A set of requirements are defined, and a system, aircraft mold line, or propulsion arrangement, depending on the particular focus of interest, is established. Trade studies that use analysis and simulation of the total system are used to determine the optimal design for meeting the requirements. Frequent configuration changes are typical in this stage of aircraft design, which cause frequent and significant changes to various subsystem models, such as aerodynamics, propulsion, actuators, and so forth. Unfortunately these aircraft design characteristics can complicate the use of a six-degree-of-freedom (6-DOF) simulation. Changes to the various subsystem models often are significant enough to require modification and possible redesign of the control laws. Frequent changes to the models, however, allow little time to make these control law modifications.

Developing a generic set of control laws that are independent of some of the most significant influences on aircraft dynamics, such as aerodynamics and propulsion, could eliminate part of the problem of using 6-DOF simulation in the preliminary design phase. These control laws could allow a 6-DOF simulation as a rapid prototyping tool, supplying usable control laws with minimal modification for any aircraft configuration. The simulation could then quickly be adapted for typical preliminary design phase tasks such as actuator bandwidth sizing, aerodynamic uncertainty sensitivity studies, performance trade studies, and mission planning.

Dynamic inversion is a control law methodology that could be developed into the desired generic set of control laws. Figure 1 shows the utility of this methodology across four linearized aerodynamic aircraft models (ranging from a lifting body (X-38 aircraft) to fighter aircraft to airbreathing hypersonic vehicles) across four flight conditions (ranging from subsonic to hypersonic). Figure 1 demonstrates that the pitch rate response to a given stick input is the same, regardless of the aircraft type or flight condition. This phenomenon occurs because the dynamic inversion methodology incorporates an aerodynamic model of the aircraft. The model, which can be stable or unstable, is inverted and used to cancel the bare airframe dynamics, allowing the control law designer to define the desired dynamics. In this sense the control laws and the desired vehicle response are independent of the aerodynamics, provided that the model used in the control law algorithm is valid.

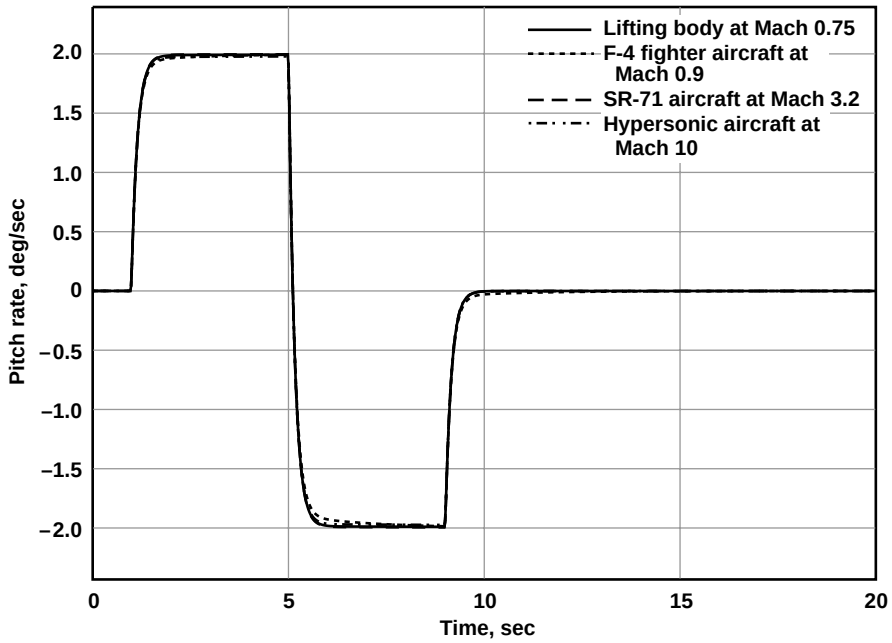

Figure 1. Pitch rate response of four linearized aerodynamic aircraft models.

Researchers at the NASA Dryden Flight Research Center (Edwards, California) recently evaluated a set of generic dynamic inversion control laws for a 6-DOF simulation environment. Two types of dynamic inversion methodologies were investigated. Reference 1 discusses one type, nonlinear dynamic inversion (NDI), which incorporates full-state nonlinear equations[2] into the control law architecture. Although dynamic inversion is primarily an inner-loop function, outer-loop functions such as guidance in relation to the NDI were investigated. The other type of dynamic inversion methodology is a simplified approach to NDI, described in reference 3 as simplified dynamic inversion (SDI). This approach uses state acceleration feedback and aerodynamic surface effectiveness estimates to perform the dynamic inversion cancellation of a full nonlinear aerodynamic model. This approach was extended in the NASA Dryden investigation with the addition of a feature that allows rapid and easy modification to the control variables that the pilot commands. The primary focus of the SDI investigation was inner-loop dynamics and pilot-in-the-loop control.

This report describes the generic implementation of SDI into 6-DOF real-time simulations of an airbreathing hypersonic vehicle at Mach 6, and a twin engine, high-performance fighter aircraft at a subsonic flight condition. Included in the generic control law architecture is a direct allocation scheme to command aircraft effectors. With minimal change to the control laws, the generic utility of SDI is demonstrated through a comparison of the inner-loop dynamics between the two simulations. The ability to easily modify control variables that the pilot commands is demonstrated. Algorithm modifications necessary to run the simulation within real-time timing constraints, and the implications of these modifications on flying qualities, are discussed. A research pilot's handling qualities evaluation of the fighter aircraft simulation also is presented.

II. Simulation and Aircraft Description

NASA Dryden has developed a common simulation platform that is used for all 6-DOF simulations originating at the center. It is capable of simulating wide ranges of aircraft and includes basic analysis tools integrated into the simulation environment. The simulation platform can run in both real-time and batch modes to allow pilot-in-the-loop evaluations and analysis from the engineer's desktop. Pilot-in-the-loop evaluations use a fixed-base, real-time simulation with standard stick and rudder pedal inceptors for pilot controls, head-up display, cockpit flight instruments, and external real-time visual imagery. Round-Earth nonlinear equations of motion are utilized. A standard architecture for subsystems is included in the simulation. The control system described in this report uses the standard architecture so that as new simulations are developed, modifications to the control system are not necessary. Specifically, the control laws require common access to the simulation aerodynamic database.

Two distinctly different aircraft simulations were used to test the utility of the control system. An airbreathing hypersonic vehicle in the conceptual design phase and a well-established twin-engine, supersonic fighter aircraft were evaluated. Both aircraft are capable of pilot-in-the-loop simulation. The hypersonic aircraft was evaluated at approximately Mach 6, at which point the simulation models are relevant. The aircraft is controlled in the longitudinal and lateral axes by symmetrically and differentially deflected wings, respectively. Directional control is maintained by symmetrically deflected rudders. Interestingly, in airbreathing hypersonic vehicles, the shape of the fuselage acts as an inlet and a nozzle for the engine. This unique characteristic causes a coupling between engine thrust and pitching moment.

The fighter aircraft was evaluated across the full flight envelope (subsonic, transonic, and supersonic) at normal and unusual attitudes to extensively test the robustness of the control system. The aircraft has 12 effectors consisting of an inboard and outboard leading edge flap on each wing, ailerons, a trailing edge flap on each wing, a rudder on each of the twin tails, and stabilators. Table 1 summarizes the basic characteristics of each aircraft.

Table 1. Comparison of basic aircraft characteristics.

	Fighter aircraft	Hypersonic aircraft
Total weight, lb	32,000	4,800
Length, ft	56	16
Reference wing area, ft^2	400	74
Speed range, Mach	0.3–1.8	4–8

III. Control Law Architecture

The objective was to design a control law framework that minimizes the number of changes required to implement the control law software in any given simulation. Furthermore, gain changes should be minimized when simulation models are updated during conceptual or preliminary design. To accomplish these objectives, dynamic inversion was chosen as a basic building architecture for the control system. A control allocation scheme was implemented to allow for the use of any number of control effectors.

Figure 2 provides an overview of the control law architecture. The control system is broken into four major sections: the input and output interfaces, SDI control section, control allocator, and B-matrix estimation (BEST) algorithm. The input and output interfaces are used to connect the control system with the simulation and to access simulation models required by dynamic inversion. All required simulation parameters, outputs from the control system, and external commands must pass through these interfaces. The interfaces were established in this manner to allow the control law subroutines to be used with any NASA Dryden simulation with minimal changes. The SDI control allocator and BEST algorithm are described in detail in the remainder of this section.

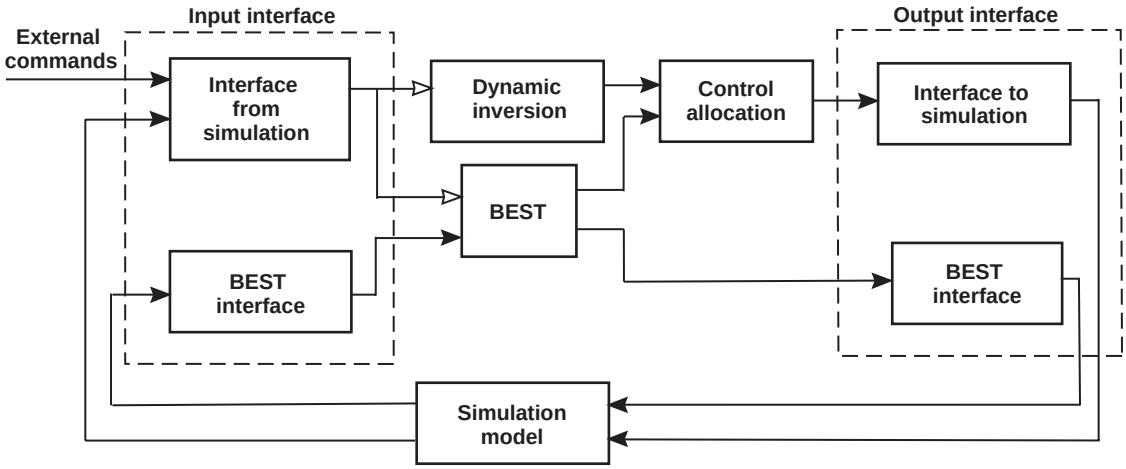

Figure 2. Overview of generic control law architecture.

A. Simplified Dynamic Inversion (SDI) Background

The objective of dynamic inversion is to calculate a control surface deflection such that the bare airframe dynamics are cancelled, allowing the control system designer to establish the desired dynamics. The following equations are used to calculate the control surface deflection, where m designates the state space representation of the modeled bare airframe, and D_m is assumed to be zero for simplification:

$$\dot{x} = A_m\, x + B_m\, u_{cmd} \tag{1}$$

$$y = C_m\, x \tag{2}$$

The dynamic inversion philosophy is that the desired dynamics ($\dot{cv}$) equals the aircraft response, so

$$\dot{cv} = \dot{y} = C_m\, \dot{x} \tag{3}$$

Substituting the equation for $\dot{x}$ (Eq. (1)) into Eq. (3) yields

$$\dot{cv} = C_m \; A_m \; x + C_m \; B_m \; u_{cmd} \tag{4}$$

Then, applying the surface command through the actuator representation, *ACT*,

$$u = ACT \left[u_{cmd} \right] \tag{5}$$

Solving for u_{cmd} in Eq. (4) and substituting it into Eq. (5) yields the following:

$$u = ACT \left\{ \left[C_m \; B_m \right]^{-1} \left[\dot{cv} - C_m \; A_m \; x \right] \right\} \tag{6}$$

This equation represents the part of the dynamic inversion method that calculates the control surface deflections to cancel the bare airframe dynamics, assuming invertible matrices. If the modeled dynamics accurately represent the actual aircraft (that is, $A = A_m$, $B = B_m$, and $C = C_m$), the realized aircraft dynamics are reduced to

$$y = \int \dot{cv} \; dt \tag{7}$$

Figure 3 illustrates the dynamic inversion approach and shows the reduction of the aircraft dynamics described in Eq. (7).

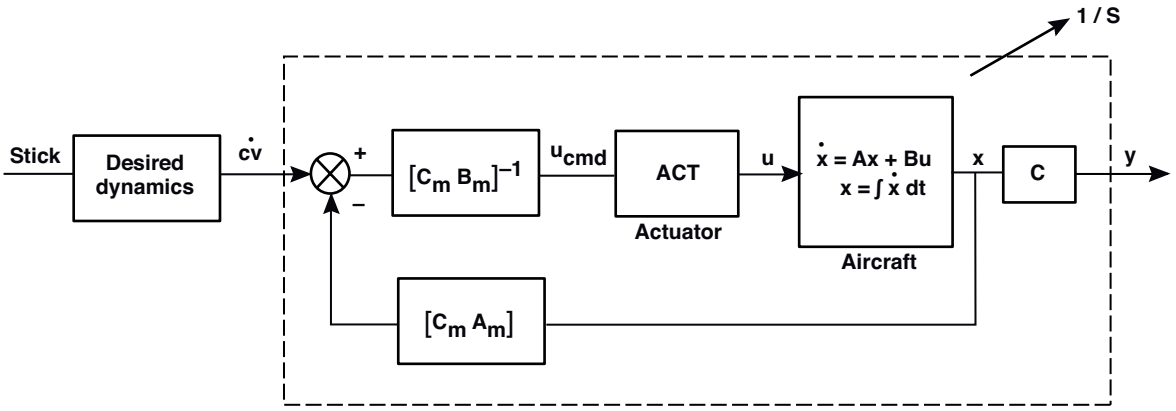

Figure 3. Dynamic inversion approach.

The SDI approach[3] achieves the same equation for control surface deflection (Eq. (6)) through the use of acceleration and surface position feedbacks instead of the modeled A matrix. Figure 4(a) illustrates the SDI approach. This diagram can be rewritten as shown in Fig. 4(b), and by means of that diagram, the control surface calculation required to cancel the airframe dynamics is

$$u_{cmd} = \left[C_m \; B_m \right]^{-1} \left[\dot{cv} - \dot{y} \right] + u \tag{8}$$

$$\dot{y} = \left[C \; A \right] x + \left[C \; B \right] u \tag{9}$$

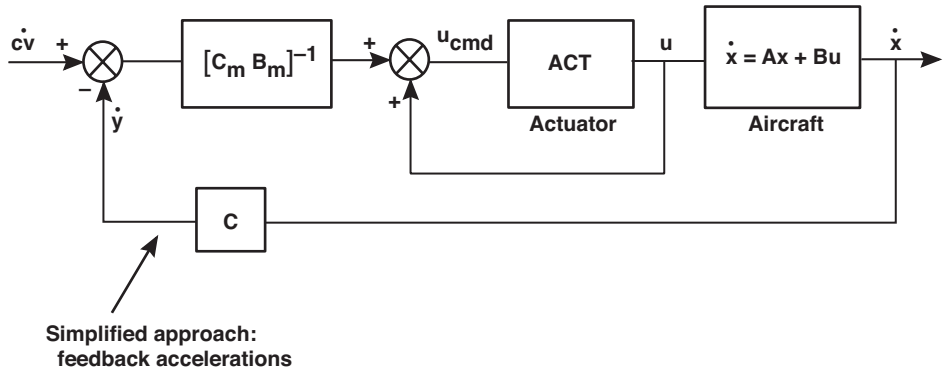

a) SDI approach.

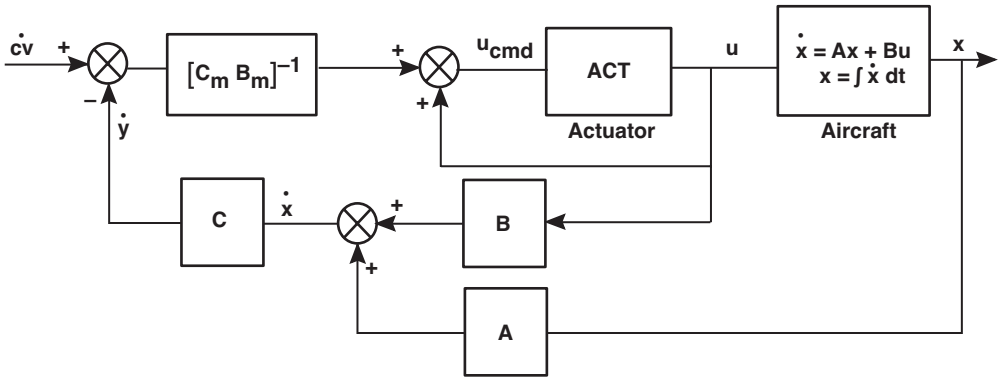

b) Equivalent SDI approach.

Figure 4. Simplified dynamic inversion (SDI) concept.

Substituting the equation for $\dot{y}$ (Eq. (9)) into Eq. (8) yields

$$u_{cmd} = \left[C_m \; B_m\right]^{-1} \left\{\dot{cv} - \left[C \; A\right] x - \left[C \; B\right] u\right\} + u \tag{10}$$

Assuming that the modeled aircraft is accurate ($A = A_m$, $B = B_m$, $C = C_m$), the $[C_m \; B_m]^{-1}$ $[C \; B]$ term becomes the identity matrix, and Eq. (10) reduces to

$$u_{cmd} = \left[C_m \; B_m\right]^{-1} \left[\dot{cv} - C_m \; A_m \; x\right] \tag{11}$$

Substituting Eq. (11) into the equation for surface position, Eq. (5) (shown in Fig. 4(b)), yields the same equation for the control surface deflection as calculated for the dynamic inversion approach (Eq. (6)).

B. Simplified Dynamic Inversion (SDI) Implementation

Figure 5 illustrates the SDI architecture implemented into the three axes for the simulations. Although the inversion step shown in Fig. 5 was implemented within the control allocator, it is included here to reflect Eq. (11). The diagram also exhibits the architecture for tuning desired dynamics, represented by a stick sensitivity gain (K_{in}) and a bandwidth gain (K_{bw}). Adding control variable feedback into the architecture allowed relatively easy and quick modification to the control system command type. For example, in the longitudinal axis, nulling the control variable feedback allowed the pilot to command rates. Conversely, selecting angle of attack as the control variable allowed the pilot to make command inputs to angle of attack. In the longitudinal axis, selectable control variables were pitch rate, pitch attitude, normal acceleration, vertical speed, flightpath, rate of change of flightpath, and angle of attack. In the lateral axis, selectable control variables were bank angle, body-axis roll rate, and stability-axis roll rate. In the directional axis, the selectable control variables were sideslip, sideslip rate, lateral acceleration, and yaw rate. Figure 6 shows the results of a rudder pedal step input for the four directional control variables. The default control variables were pitch rate, body-axis roll rate, and lateral acceleration.

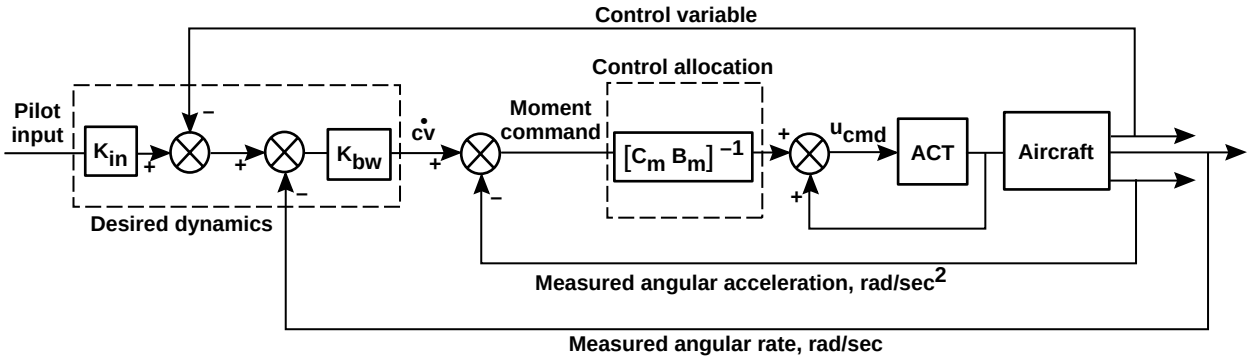

Figure 5. Simplified dynamic inversion (SDI) as implemented in the generic control laws.

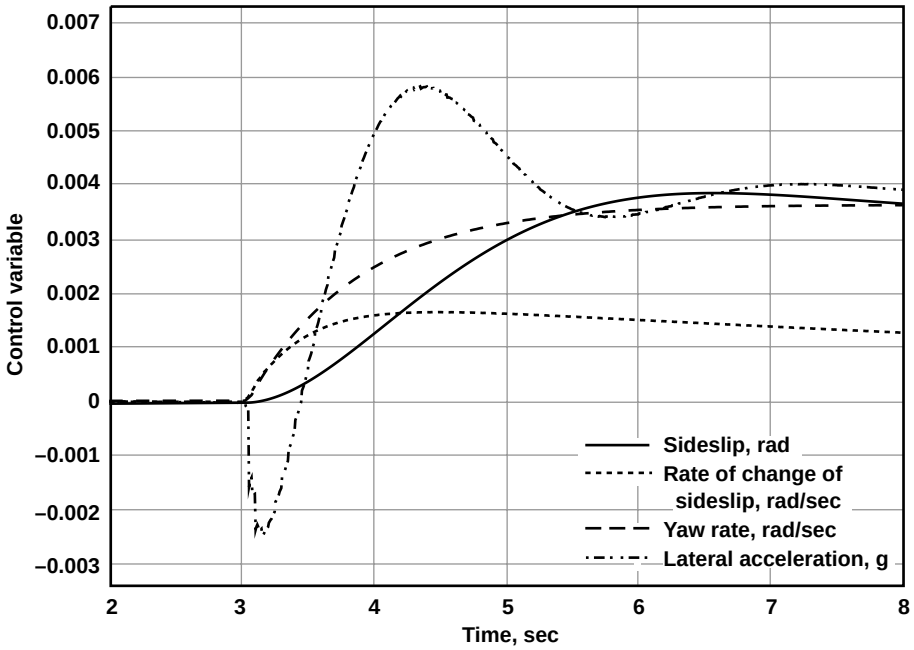

Figure 6. Responses to a step input for the four directional control variables.

Increasing the bandwidth gain, K_{bw}, increased the response time of the controller, but it required more rate from the actuator and provided more oscillatory responses. Figure 7 shows the effect for the lateral acceleration control variable when step inputs with increasing bandwidth gain were applied. Table 2 lists the nominal gains and control variables for each axis in both simulations.

Output from the SDI is a commanded moment for each axis. Although the SDI technique generally requires a surface effectiveness estimate to convert the commanded moment to a surface position command, this step was relegated to the control allocation algorithm where the B matrix was estimated.

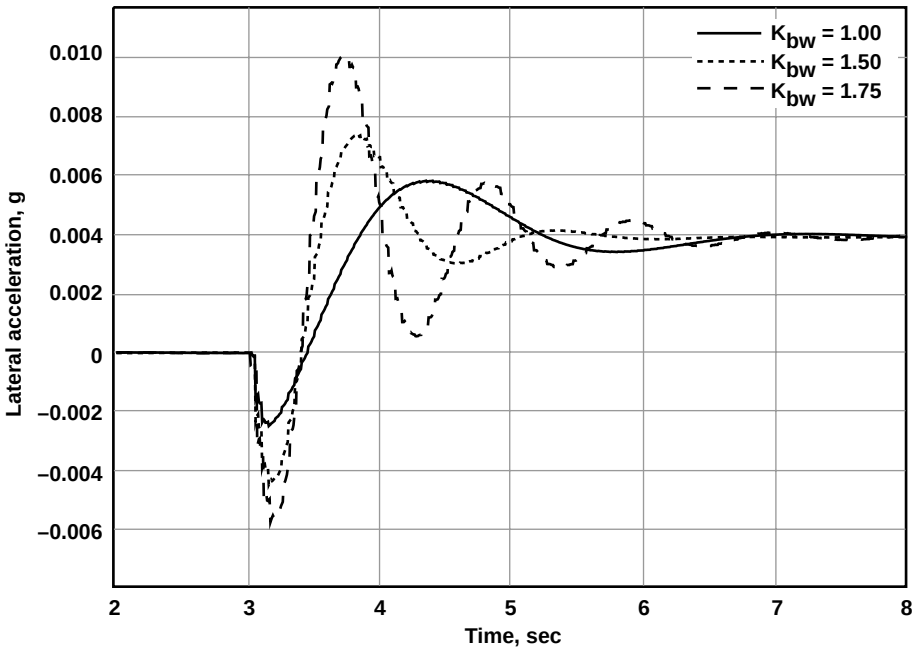

Figure 7. Responses to step inputs with varying bandwidth gains.

Table 2. Nominal gains and control variables.

Axis	Control variable	K_{in}	K_{bw}
Pitch	Pitch rate	1.0	6.0
Roll	Roll rate	10.0	6.0
Yaw	Sideslip	0.05	1.0

C. Control Allocation

The control allocation section of the control system is an algorithm taken from reference 4. The control allocator uses a model matching technique to compute a set of effector commands from a moment command input. The controller requires a model input for the aircraft, which is accomplished with a BEST algorithm. A change in nondimensional moment from the current aircraft state is commanded as input in addition to a control effector matrix and effector limits. The allocator then determines a change in effector output command, which is then summed with the current aircraft effector position to create a new effector position command to the simulation actuator model.

D. B-Matrix Estimation (BEST) Algorithm

The BEST routine outputs a linearized estimate of the effectiveness of each control effector at the current state in time as a function of control deflection. The algorithm works by cycling through all effector positions and adding a positive and negative increment to the current value of each position for a given frame. For each increment the aerodynamic model is called, and the differences in pitch, roll, and yaw aerodynamic moments are calculated. The difference in each aerodynamic moment is essentially an estimate of the control surface effectiveness for that effector in that frame.

Effort was devoted to developing the BEST routine such that it would be compatible with current simulation architecture and fit within a real-time simulation frame. To determine an appropriate balance between accuracy and speed, modifications to the algorithms were attempted. Initially the BEST routine updated the effectiveness for all surfaces in a given frame. Computational requirements for this approach were too stringent, however, to fit within the simulation integration step for the fighter aircraft simulation. For a point of reference, the fighter aircraft simulation ran simulation and visual graphics software on a SGI® ONYX® 2 system (Silicon Graphics, Inc., Mountain View, California) configured with eight MIPS® Technologies R12000™, 400-MHz processors (MIPS Technologies, Inc., Mountain View, California). Computational time modifications were implemented in the following order to reduce requirements:

1) Speed enhancements to the code
2) BEST update for one surface for each simulation frame
3) Assumptions on surface deflections to reduce to eight collective effectors
4) Perform half-step increments, instead of a positive and negative increment, to obtain effectiveness estimates

To limit the control surfaces to eight collective effectors, the following assumptions were imposed: slave the inboard and outboard flaps, limit the rudder to symmetric deflections only, and limit the aileron to asymmetric deflections only. Half-step estimates, in which control surface effectiveness is estimated by means of a step in only one direction, save computations by reducing the calls to the aerodynamic model, but they increase estimation errors. The direction is based on whether the rate of change of the nominal aerodynamic moment is positive or negative. If the moment is moving in a positive direction, then the BEST algorithm uses an increment that produces a positive moment. If it is moving in a negative direction, then the BEST algorithm uses an increment that produces a negative moment. A flag was implemented in the simulation to toggle between half-step estimates and full-step estimates, which uses the positive and negative increments.

Despite efforts to maintain computations within the simulation integration step, frame overruns continued. An additional effort to fit the computations within the simulation step was successful. Splitting the execution of the visual graphics and the simulation modeling onto two computers reduced the overall computational time of the simulation and allowed the entire computation to fit within the simulation integration step. The additional computer, a Sun system (Sun Microsystems, Inc., Santa Clara, California) configured with four SPARC® V9, 900-MHz processors (SPARC International, Inc., Campbell, California), ran the simulation software, and the SGI® system ran the visual graphics. Control law changes made to the fighter aircraft simulation for timing considerations were then incorporated into the hypersonic aircraft simulation to maintain code consistency.

Figure 8 compares the actual computational time to the simulation frame rate requirement. The most significant time savings resulted from surface modifications, which included the BEST update for one surface for each simulation frame, and the surface assumptions that reduced the number of effectors (steps 2 and 3 described previously).

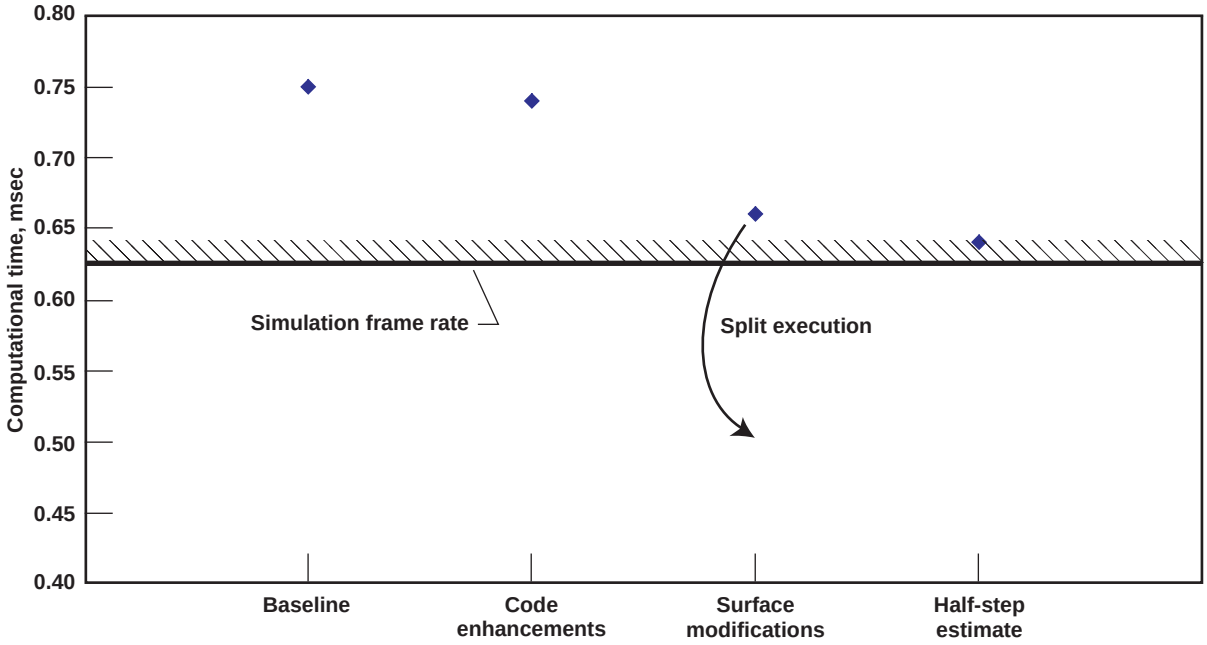

Figure 8. Comparison of actual computational time to simulation frame rate.

E. Applicability to the Flight Environment

Although the purpose of this report is to discuss the application of the SDI approach to the simulation environment, two significant challenges that arise when the SDI method is applied in flight should be mentioned. The first challenge is to estimate the surface effectiveness. To estimate the surface effectiveness, either an onboard aerodynamic model or a real-time parameter estimation technique must be implemented in the SDI algorithm. An onboard aerodynamic model would have to be simplified to function in a real-time environment and thus is susceptible to errors. A parameter estimation technique would require a significant developmental process to verify that it will accurately function in a real-time environment. The second challenge is to obtain acceleration feedback. Whether rotational accelerometers can produce a signal that is accurate, clean, and reliable enough for use as a feedback signal in a control law is not known. Data from embedded global positioning systems and inertial navigation systems, however, potentially could provide a clean, accurate signal. These challenges hinder the application of the SDI method to the flight environment. Reference 5 discusses efforts to develop a similar SDI method that might not be subject to these challenges.

IV. Evaluation of Handling Qualities

To determine whether general handling quality deficiencies of the generic control laws exist and to demonstrate the application of the control laws for representative piloting tasks, the handling qualities of the fighter aircraft simulation were investigated by a research pilot. Three tasks, representative of fighter tasks, were defined for this purpose: offset acquisition, air-to-air tracking, and offset landing. The offset acquisition and air-to-air tracking tasks were up-and-away tasks. The offset landing task was an approach and landing task in a power approach configuration. General task performance guidelines were used so that the pilot could provide insight on the handling qualities.

During the offset acquisition task, a visual target was provided at the same altitude, heading, and airspeed as those of the simulation aircraft, at a range of 1000 ft. The task was conducted with the target aircraft at either a lateral or vertical offset. Figure 9 shows the starting condition (from the pilot's perspective) for the lateral offset. The piloting task was to acquire the offset target and hold it within the inner of two concentric pippers for 3 sec. After 3 sec the pipper would turn from green to red and the target aircraft would offset to the opposite side, allowing the pilot to reacquire it. The desired performance guideline was to acquire the target aircraft within 3–4 sec from the time of the offset with two or less overshoots.

The air-to-air target tracking task had the same setup as that of the offset acquisition task, but without the offset. The target aircraft would enter a 3-*g* turn and hold it for 45 sec, at which time the aircraft would reverse direction. The piloting task was to acquire the target aircraft within the inner pipper.

The offset landing task began near the final approach with the airplane (configured for a power approach) on the same heading as that of the runway but offset by approximately 300 ft. The pilot would maintain constant altitude until the pipper flashed. At this time the pilot would position the aircraft on final approach with a glide slope of 3°, while still maintaining the offset. When the pipper flashed a second time the pilot would correct to the runway centerline and attempt to touch down with the main gear on an aim point located on the runway. Figure 10 shows approximately the pilot perspective during the correction. An inner box on the runway, measuring ±250 ft from the aim point and ±25 ft from the centerline, was used as a guideline for desired performance. An outer rectangle on the runway, measuring 250 ft before and 750 ft after the aim point, and ±50 ft from the centerline, was used as a guideline for adequate performance. Similar maneuvers were performed in a previous research project and are described in detail in reference 6.

Figure 9. Offset acquisition task: starting condition with the lateral offset.

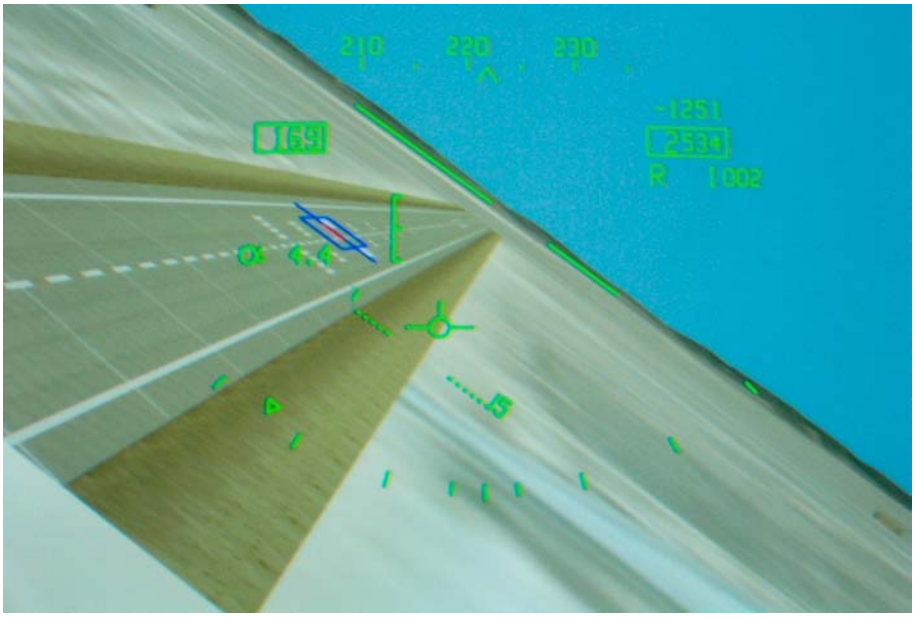

Figure 10. Offset landing task correction.

V. Results

This section examines the utility of the generic control laws based on comparisons of the responses of both simulations to open-loop inputs. A pilot opinion regarding the control laws and the ability to perform representative fighter tasks is presented. Of interest is the effect of BEST estimates on flying qualities when the half-step algorithm is used.

A. Open-Loop Input Evaluation

In theory the dynamic inversion control laws should produce output time histories for both simulations that are nearly identical for a given step input. To evaluate this SDI characteristic, the same step input was applied to both simulations in each of the three axes. The hypersonic aircraft simulation was conducted at Mach 5.78, and the fighter aircraft simulation was conducted at Mach 0.6. The control variables for the two simulations were body-axis roll rate, pitch rate, and sideslip. Nominal gains were used in both simulations. Figure 11 shows a time history comparing the control variables for each axis step input for the two simulations.

Note that the control variable responses are very similar despite the considerable disparity in aerodynamic configuration and flight condition. These results imply that the SDI technique worked as intended and the bare airframe dynamics were appropriately cancelled. For the pitch rate, the hypersonic aircraft simulation had a slightly slower response time. This response was traced to the associated coupling between engine thrust and pitching moment, a characteristic of hypersonic airbreathing engines. A second set of step responses from the hypersonic aircraft simulation, without the engine model pitching moment contribution, was recorded (Fig. 11). This pitch rate response improved the match with the fighter aircraft response.

In addition to the step inputs, frequency sweeps were applied to both simulations. The same conditions and control variables used in the step inputs were used in the frequency sweeps. The sweeps ranged in frequency from 0.1 rad/sec to 50 rad/sec. Pitch-rate-to-stick and roll-rate-to-stick frequency responses were generated for the two simulations. Figures 12 and 13 compare the frequency responses for pitch rate and roll rate, respectively. The frequency responses generally resemble first-order responses. From a handling qualities perspective a first-order roll rate response is favorable. For the pitch axis, however, a first-order pitch rate response might be less favorable.

Good agreement exists between the two simulations for both the pitch rate and roll rate frequency responses to approximately 10 rad/sec. At that point the comparisons show some deviations, particularly in the phase plot. To determine where this mismatch originates, the phase difference between the left wing actuator of the hypersonic aircraft and the left stabilator actuator of the fighter aircraft was added to the phase of the fighter aircraft frequency response. The results indicate a much improved frequency response match, as shown in Figs. 12 and 13, which implies that the phase difference primarily is a result of differing actuator models between the two simulations.

To document the stability margin robustness for this type of controller, a frequency sweep was inserted into both simulations at the inner-loop error signal for each axis.[7] Open-loop frequency responses were then generated. Figure 14 shows the pitch axis frequency response with the stability margin calculation superimposed. The similarity in the frequency responses between the two aircraft is noted for frequencies below the actuator break frequency. The roll and yaw axes frequency responses (not shown) exhibit similar characteristics. The gain and phase margins for each axis in the two simulations show a large degree of robustness (table 3).

Table 3. Comparison of stability margins for the two simulations.

Axis	Fighter aircraft (gain and phase)	Hypersonic aircraft (gain and phase)
Pitch	10 dB / 70°	17 dB / 85°
Roll	21 dB / 70°	16 dB / 80°
Yaw	30 dB / 70°	32 dB / 90°

This open-loop evaluation emphasizes the generic utility of the SDI control laws. Two distinctly different aircraft models were manipulated to provide the same responses with a significant amount of stability robustness.

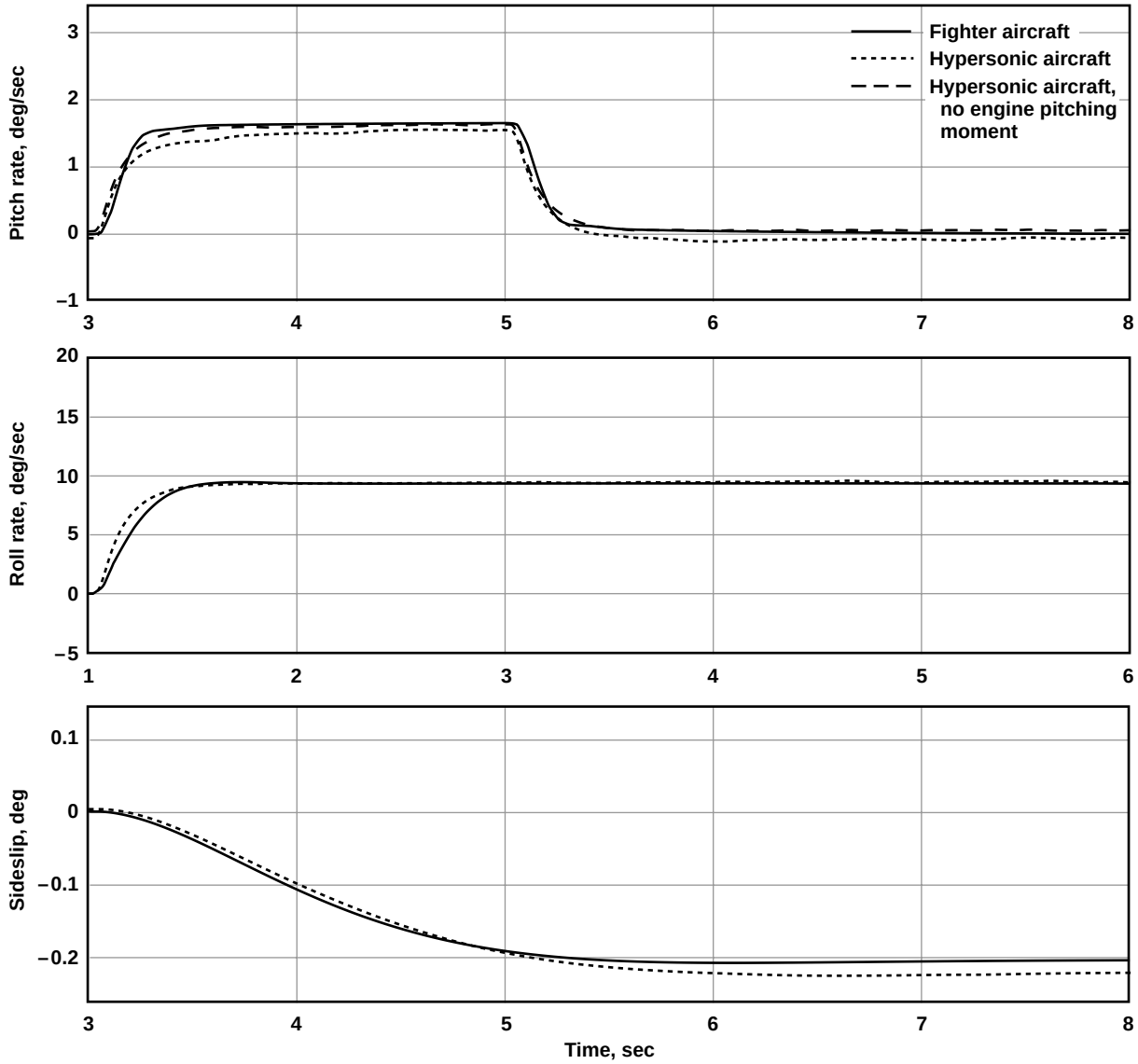

Figure 11. Comparison of fighter and hypersonic aircraft responses to a step input.

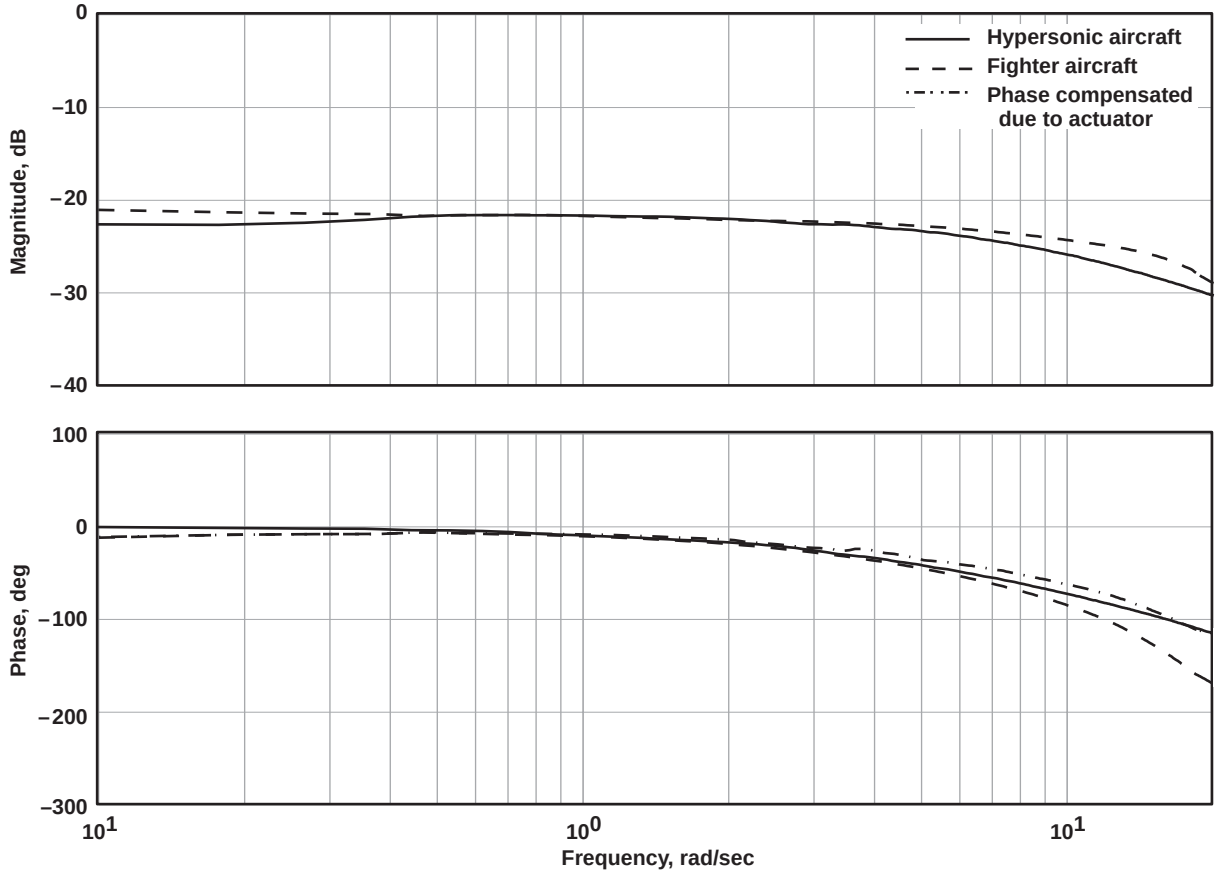

Figure 12. Comparison of pitch-rate-to-stick deflection frequency responses.

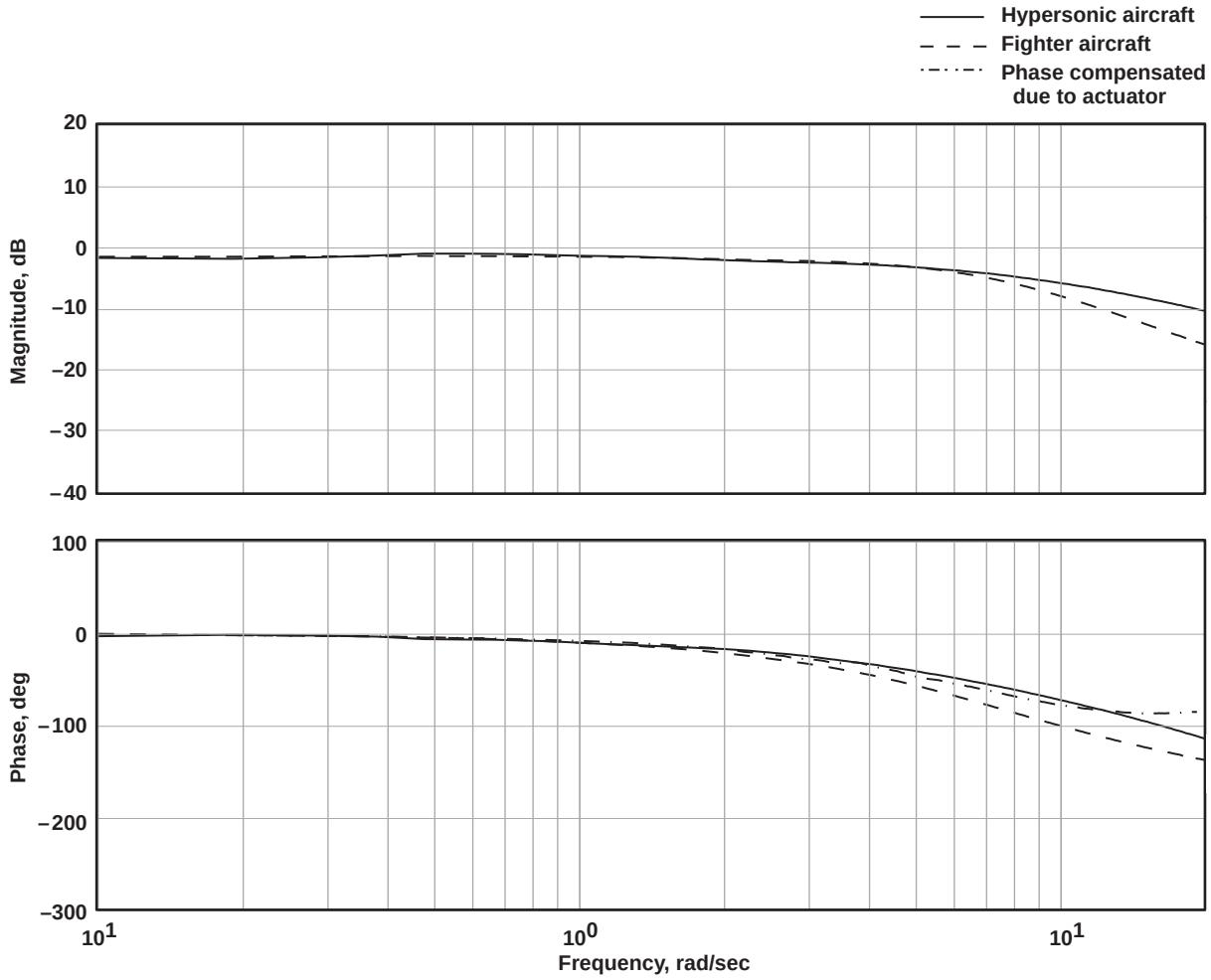

Figure 13. Comparison of roll-rate-to-stick deflection frequency responses.

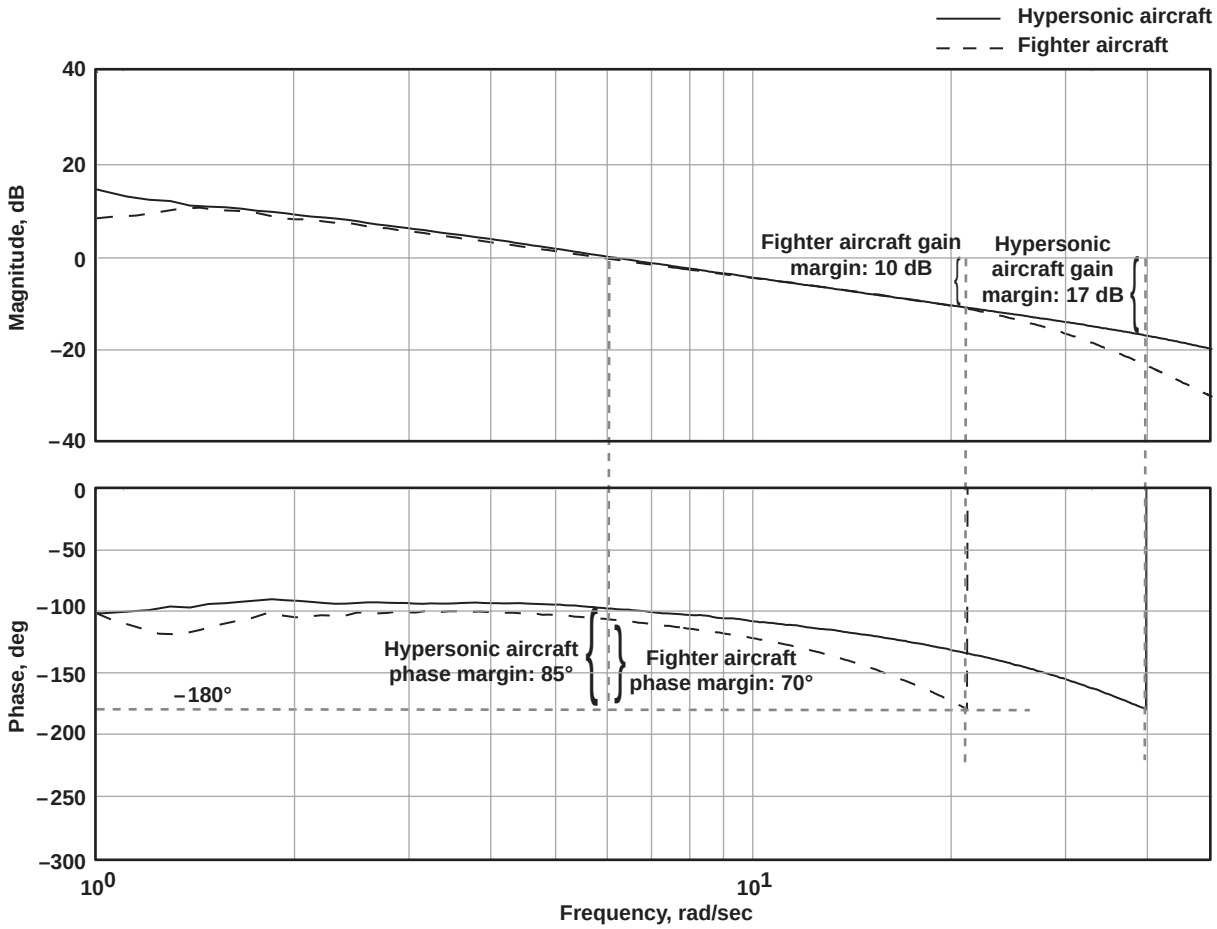

Figure 14. Comparison of pitch axis open-loop frequency responses.

B. Pilot Evaluation of Handling Qualities

To evaluate the handling qualities of the SDI control laws for representative fighter tasks, a research pilot flew the three tasks described previously (offset acquisition, air-to-air tracking, and offset landing). With the exception of the directional control variable, the control variables and gains were essentially nominal. For most of the maneuvers evaluated by the pilot, the directional control variable was sideslip.

The pilot commentary for the offset acquisition task indicates that for the lateral and vertical offsets, the airplane was clearly satisfactory without need for improvement. The following comments concerning the lateral offset task are representative:

> Airplane is easily moved to acquire inner circle in about 3 seconds. If you're more aggressive to about 1.5 to 2 seconds then you may generate one overshoot. If you are less aggressive in the 3 or 4 second range it is very easy to generate no overshoots. No PIO tendencies, no coupling between pitch and roll.

For the air-to-air tracking task, however, the comments are not as favorable. Attempting to fine track caused directional oscillations in the pipper that created difficulty in stabilizing the pipper on the target aircraft. The difficulty noted by the pilot is apparent in the time histories (Fig. 15). The pipper acquisition marker represents the status of the target aircraft relative to the inner pipper. When the target was inside the pipper the marker toggled to a value of two. In this maneuver the pilot was continually attempting to track the target aircraft, as shown in the oscillatory lateral stick time history. Sideslip oscillations were induced, which occurred at a frequency of approximately 1.25 rad/sec, and caused the pipper to swing back and forth through the target. The oscillations created difficulty for the pilot in stabilizing the pipper on the target. As a result, the target was acquired for only brief segments of time. The maneuver was repeated when the directional control variable was switched to lateral acceleration. The following comments resulted:

> Much better characteristics. Still a slight tendency for the pipper to slide, as noticed when using beta feedback, but task is much more doable. Similar to task when using [the standard airplane] control laws.

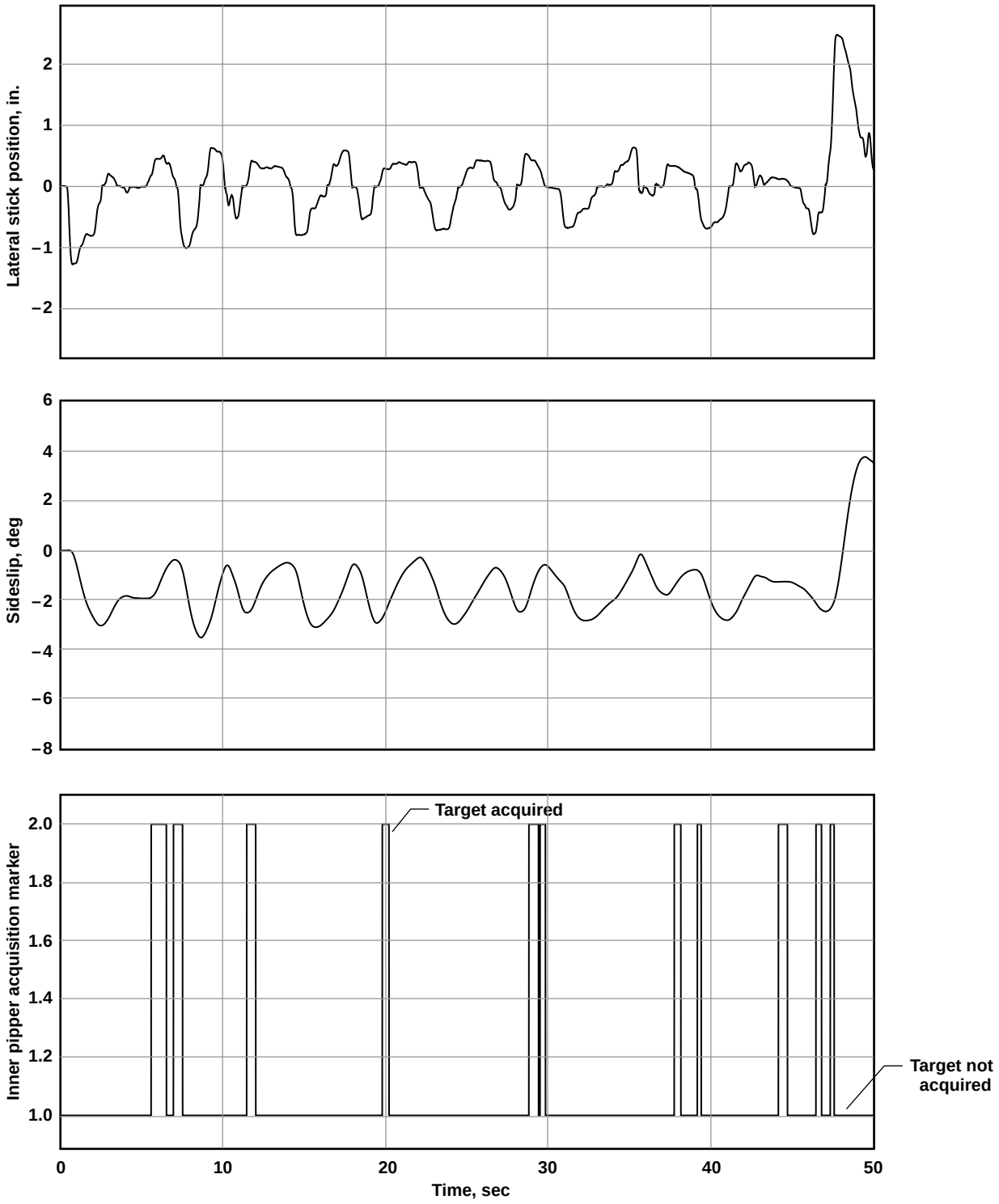

Figure 15. Time history of air-to-air tracking task with sideslip as the control variable.

The pilot commentary indicates that the aircraft was satisfactory without improvement with only some minor deficiencies. The ability to perform the task significantly improved. The acquisition marker (Fig. 16) indicates that the target was inside the inner pipper for a longer duration than when the sideslip control variable was used. Furthermore, this sideslip time history shows much better damping than the sideslip time history from Fig. 15.

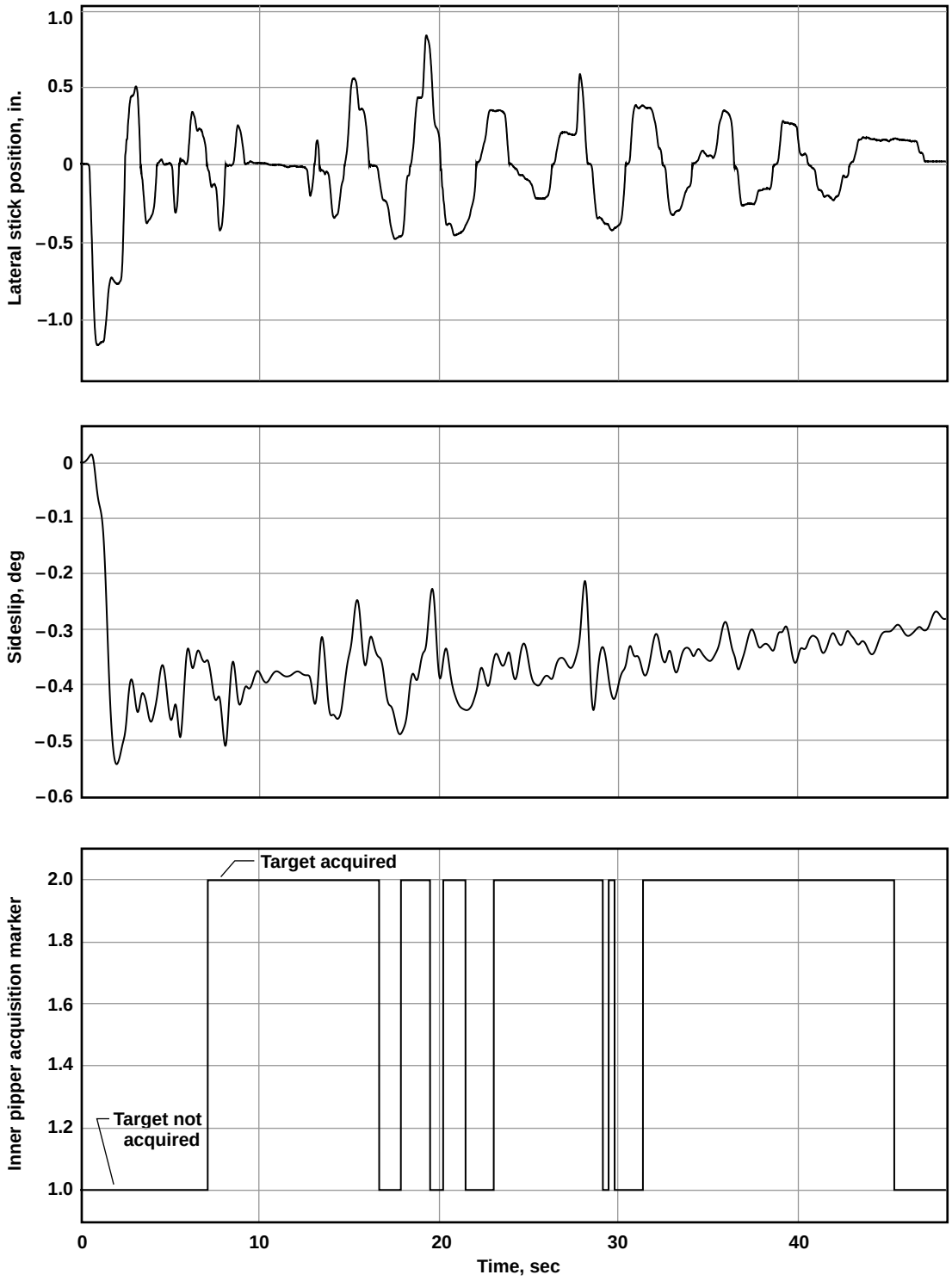

Figure 16. Time history of air-to-air tracking task with lateral acceleration as the control variable.

Comments concerning the offset landing task, when lateral acceleration was used as the control variable, indicate that the directional characteristics were similar to those of the air-to-air tracking task. In this task, however, considerable effort was necessary to perform the task within adequate guidelines.

Overall, the pilot was able to perform the representative fighter tasks. Through this evaluation, the utility of the SDI control laws was validated, and the quality of the response characteristics of the SDI control laws was documented. Furthermore, the usefulness of easily modifiable control variables (to fine tune the handling qualities) was demonstrated.

C. Implications on Flying Qualities Resulting From Half-Step B-Matrix Estimates

A feature of the SDI control laws is the ability to use half-step B-matrix estimates to save computational time. This feature had been considered beneficial for cases in which using a full-step estimate would cause the real-time computational time to exceed the integration timeframe of the simulation.

Using half-step estimates, however, would introduce errors into the B-matrix estimates, especially during highly dynamic maneuvering, and thus could produce some negative implications on flying qualities. Figure 17 shows the response of a frequency sweep, ranging from 0.1 to 50 rad/sec, in the pitch axis in which full-step and half-step estimates were used. A transient can be seen in the angle-of-attack data at approximately 55 sec (corresponding to a frequency of approximately 44 rad/sec). This transient exemplifies the type of undesirable flying characteristic that can result from the half-step B-matrix estimation. These undesirable characteristics were even more dramatic when a divergent oscillation developed while the air-to-air tracking task was executed with the half-step estimation. Therefore, half-step estimation of the B matrix is recommended only when the real-time requirement of the simulation cannot be met, in which case only moderate maneuvering should be performed.

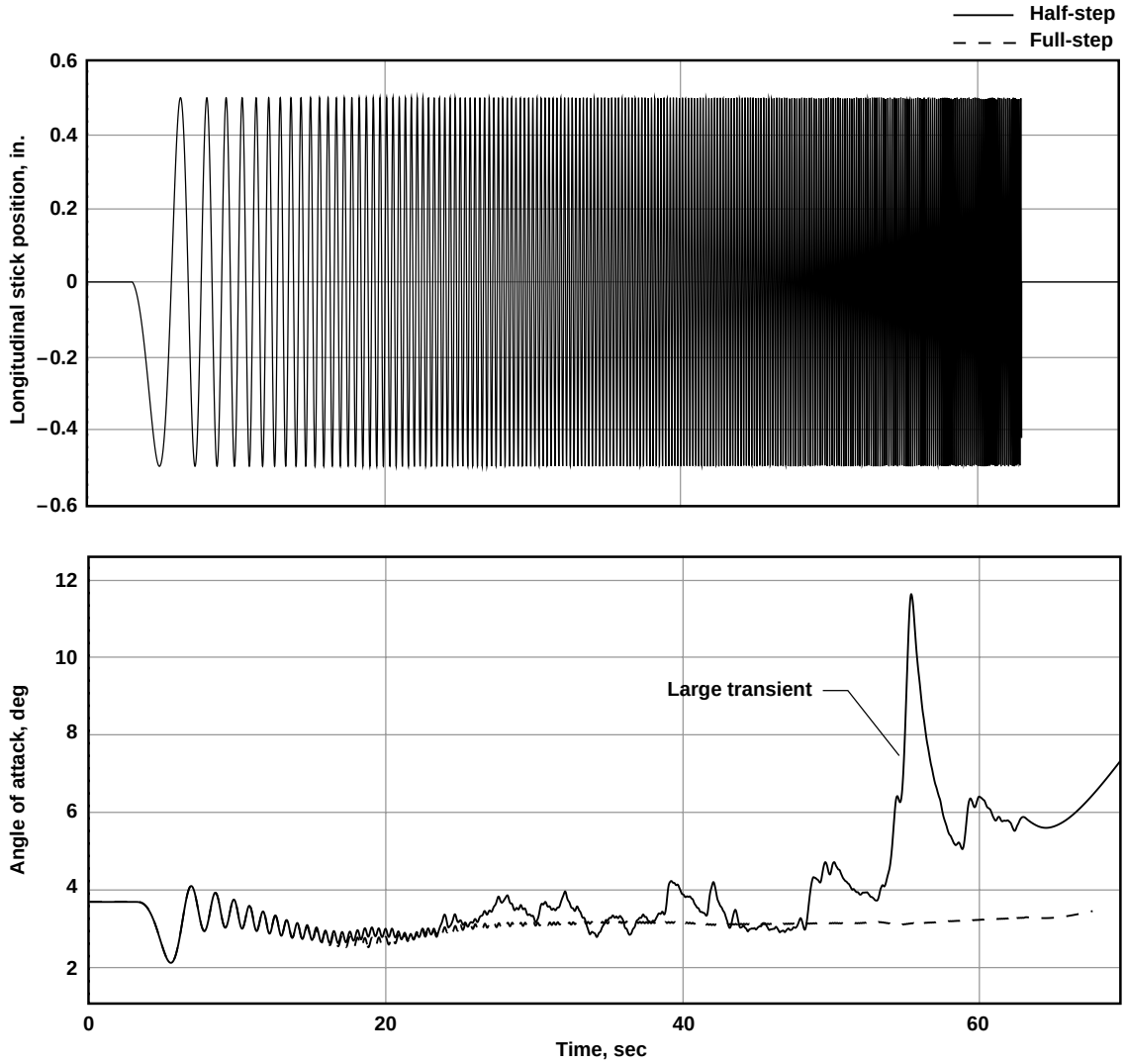

Figure 17. Comparison of frequency sweep responses in which half-step and full-step estimates were used.

VI. Conclusions

Researchers at the NASA Dryden Flight Research Center developed a set of generic dynamic inversion control laws for a six-degree-of-freedom simulation environment to aid in aircraft design in the preliminary, conceptual stages. The generic implementation utilizes a simplified dynamic inversion (SDI) approach, which uses state acceleration feedback and surface effectiveness estimates to perform the dynamic inversion cancellation of the bare airframe dynamics. The SDI control laws primarily were developed for the real-time, pilot-in-the-loop simulation environment, and some modifications to the algorithm were necessary for the simulation to run within real-time timing constraints. A feature was added to the SDI algorithm that allows quick and easy modification to the control variables that the pilot commands.

The SDI algorithm was implemented in two simulations of two distinctly different aircraft: an airbreathing hypersonic vehicle and a high-performance twin engine fighter aircraft. With minimal changes to the control laws, the generic utility was validated by demonstrating, for a given open-loop input, a match between the hypersonic aircraft simulation response at Mach 5.78 and the fighter aircraft simulation response at Mach 0.6. A stability analysis for the two simulations indicates that the control laws are robust. A research pilot considered the handling qualities of the fighter aircraft simulation closed-loop dynamics to be satisfactory without improvement for up-and-away tracking tasks. Although considerable effort was required, the pilot was able to perform offset approach and landing tasks within adequate guidelines. Through this evaluation, the ability to perform representative fighter tasks was demonstrated, and the ability to quickly modify control variables was proven to be useful for fine-tuning the handling qualities. One modification to the algorithm, however, which estimated surface effectiveness based on a technique designed to reduce computational time, produced undesirable flying qualities.

References

[1]Cotting, M. C., and Cox, T. H., "A Generic Guidance and Control Structure for Six-Degree-of-Freedom Conceptual Aircraft Design," AIAA-2005-0032, 2005.

[2]Honeywell Technology Center, Lockheed Martin Skunk Works, and Lockheed Martin Tactical Aircraft Systems, "Application of Multivariable Control Theory to Aircraft Control Laws, Final Report: Multivariable Control Design Guidelines," WL-TR-96-3099, Flight Dynamics Directorate, Wright Laboratory, Air Force Materiel Command, Wright-Patterson Air Force Base, Ohio, May 1996.

[3]Smith, P. R., "A Simplified Approach to Nonlinear Dynamic Inversion Based Flight Control," AIAA-98-4461, 1998.

[4]Bordignon, K. A., and Durham, W. C., "Closed-Form Solutions to Constrained Control Allocation Problem," *Journal of Guidance, Control, and Dynamics,* Vol. 18, No. 5., Sept.–Oct. 1995.

[5]Bacon, B. J., and Ostroff, A. J., "Reconfigurable Flight Control Using Nonlinear Dynamic Inversion with a Special Accelerometer Implementation," AIAA-2000-4565, 2000.

[6]Mayer, J., and Cox, T. H., "Evaluation of Two Unique Side Stick Controllers in a Fixed-Base Flight Simulator," NASA TM-2003-212042, 2003.

[7]Bosworth, J. T., "Flight-Determined Longitudinal Stability Characteristics of the X-29A Airplane Using Frequency Response Techniques," NASA TM-4122, 1989.